JOURNAL OF THE AMERICAN COLLEGE OF CARDIOLOGY
© 2017 BY THE AMERICAN COLLEGE OF CARDIOLOGY FOUNDATION
PUBLISHED BY ELSEVIER

VOL. 70, NO. 1, 2017
ISSN 0735-1097/$36.00
http://dx.doi.org/10.1016/j.jacc.2017.05.028

Arterial Remodeling After Bioresorbable Scaffolds and Metallic Stents

Patrick W. Serruys, MD, PhD,[a] Yuki Katagiri, MD,[b] Yohei Sotomi, MD,[b] Yaping Zeng, MD, PhD,[c] Bernard Chevalier, MD,[d] René J. van der Schaaf, MD, PhD,[e] Andreas Baumbach, MD, PhD,[f] Pieter Smits, MD,[g] Nicolas M. van Mieghem, MD, PhD,[c] Antonio Bartorelli, MD,[h] Paul Barragan, MD, PhD,[i] Anthony Gershlick, MD, PhD,[j,k] Ran Kornowski, MD,[l] Carlos Macaya, MD,[m] John Ormiston, MD,[n] Jonathan Hill, MD,[o] Irene M. Lang, MD,[p] Mohaned Egred, MBChB, MD,[q] Jean Fajadet, MD,[r] Maciej Lesiak, MD,[s] Stephan Windecker, MD, PhD,[t] Robert A. Byrne, MBBCh, PhD,[u] Lorenz Räber, MD,[t] Robert-Jan van Geuns, MD, PhD,[c] Gary S. Mintz, MD,[v] Yoshinobu Onuma, MD, PhD[c]

ABSTRACT

BACKGROUND Although previous observational studies have documented late luminal enlargement and expansive remodeling following implantation of a bioresorbable vascular scaffold (BVS), no comparison with metallic stents has been conducted in a randomized fashion.

OBJECTIVES This study sought to compare vessel remodeling patterns after either Absorb BVS or Xience metallic drug-eluting stent (DES) implantation (Abbott Vascular, Santa Clara, California) and determine the independent predictors of remodeling.

METHODS In the ABSORB II randomized trial, 383 lesions (n = 359) were investigated by intravenous ultrasound both post-procedure and at 3-year follow-up. According to vessel and lumen area changes over 3 years, we categorized 9 patterns of vessel remodeling that were beyond the reproducibility of lumen and vessel area measurements.

RESULTS The relative change in mean vessel area was significantly greater with the BVS compared to the DES (6.7 ± 12.6% vs. 2.9 ± 11.5%; p = 0.003); the relative change in mean lumen area was significantly different between the 2 arms (1.4 ± 19.1% vs. −1.9 ± 10.5%, respectively; p = 0.031). Multivariate analysis indicated that use of the BVS, female sex, balloon-artery ratio >1.25, expansion index ≥0.8, previous percutaneous coronary intervention, and higher level of low-density lipoprotein cholesterol were independent predictors of expansive remodeling. Furthermore, in the BVS arm, necrotic core pre-procedure was an independent determinant of expansive remodeling.

CONCLUSIONS Expansive vessel wall remodeling was more frequent and intense with the BVS than the metallic DES and could be determined by patient baseline characteristics and periprocedural factors. The clinical effect of the observed lumen and vessel remodeling must be investigated in further large clinical studies to optimize the clinical outcome of patients and lesions treated by bioresorbable scaffolds. (ABSORB II Randomized Controlled Trial; NCT01425281) (J Am Coll Cardiol 2017;70:60–74) © 2017 by the American College of Cardiology Foundation.

Listen to this manuscript's audio summary by *JACC* Editor-in-Chief Dr. Valentin Fuster.

From [a]The National Heart and Lung Institute, Imperial College London, London, United Kingdom; [b]Academic Medical Center, University of Amsterdam, Amsterdam, the Netherlands; [c]ThoraxCenter, Erasmus Medical Center, Rotterdam, the Netherlands; [d]Department of Interventional Cardiology, Institut Jacques Cartier, Massy, France; [e]Onze Lieve Vrouwe Gasthuis, Amsterdam, the Netherlands; [f]Bristol Heart Institute, Bristol, United Kingdom; [g]Maasstad Hospital, Rotterdam, the Netherlands; [h]Centro Cardiologico Monzino, University of Milan, Milan, Italy; [i]Polyclinique les Fleurs, Ollioules, France; [j]Department of Cardiology, University of Leicester, Leicester, United Kingdom; [k]NIHR Leicester Cardiovascular Biomedical Research Centre, Leicester, United Kingdom; [l]Rabin Medical Center, Petah Tikva, Israel; [m]Hospital Clinico San Carlos, Universidad Complutense, Madrid, Spain; [n]Green Lane Cardiovascular Service, Auckland City Hospital, Auckland, New Zealand; [o]King's College Hospital, London, England; [p]Division of Cardiology, Department of Internal Medicine II, Medical University of Vienna, Vienna, Austria; [q]Freeman Hospital & Newcastle University, Institute of Cellular Medicine, Newcastle upon Tyne, United Kingdom; [r]Clinique Pasteur, Toulouse, France; [s]Department of Cardiology, Poznan University of Medical Sciences, Poznan, Poland; [t]Department of Cardiology, Bern University Hospital, Bern, Switzerland; [u]Deutsches Herzzentrum München, Technische Universität München, Munich, Germany; and the [v]Cardiovascular Research Foundation, New York, New York. This study was funded by Abbott Vascular. Dr. Serruys has served as a member of the advisory board for Abbott Vascular. Dr. Chevalier has served as a consultant for Abbott Vascular.

Intravascular ultrasound (IVUS) has been instrumental in the understanding of the atherosclerotic process and in the development of coronary interventional cardiology (1). Basically, IVUS defines 2 interfaces: 1) one between the flowing blood and the intima; and 2) one between the media and the adventitia. Therefore, multiple options of interaction exist among these 3 compartments, lumen, plaque-media, and adventitia. The relationship between lumen area (LA), plaque-media, and vessel area (VA) is the foundation of Glagov's principle of compensatory expansive remodeling of the external elastic membrane (2). Considering the changes in these 3 compartments, there are, conceptually, 9 possibilities of expansive or constrictive remodeling, increase or decrease in plaque-media, and increase or decrease in LA (3). Fundamental to atherosclerosis progression and regression, these interactions are also essential as vessel wall reactions to the transient barotrauma of balloon angioplasty (4–7) and the permanent or transient "scaffolding" effect of either metallic stents (8) or bioresorbable scaffolds (9).

SEE PAGE 75

The advent of bioresorbable vascular scaffolds (BVS) has prompted us to analyze the short- and long-term effect of the bioresorbable scaffolds on vessel wall dynamics, including remodeling (10). It has been hypothesized that the potential for remodeling should be more prominent than the remodeling observed with metallic stents and should lead to late lumen enlargement (11). The ABSORB II trial did not meet its coprimary endpoints: superiority in vasomotion and noninferiority in angiographic late luminal loss following implantation of the Absorb drug-eluting BVS compared with the Xience metallic drug-eluting stent (DES) (Abbott Vascular, Santa Clara, California), but it has given us the opportunity to investigate, in the context of a randomized trial, the changes of long-term vessel wall morphometry after implantation of either bioresorbable scaffolds or metallic stents.

METHODS

The ABSORB II trial was a prospective, single-blind, multicenter clinical trial that randomized patients to percutaneous coronary intervention (PCI) with placement of either Absorb bioresorbable scaffolds or Xience metallic stents in a 2:1 fashion. The trial design, the study devices, and the inclusion and exclusion criteria have been described in detail previously (12,13). As mandated by the protocol, all patients underwent documentary grayscale IVUS and backscattered radiofrequency (virtual histology [VH]) assessment before and after device implantation, as well as at 3-year follow-up. Clinical visits and blood sample analysis, including low-density lipoprotein cholesterol (LDL-C), were performed at 30 and 180 days and at 1, 2, and 3 years after the index procedure. The blood samples were analyzed by a central laboratory.

IVUS IMAGE ACQUISITION AND ANALYSIS. IVUS data were acquired with a 3.2-F, 45 MHz rotational IVUS catheter (Revolution 45 MHz, Volcano Corporation, Rancho Cordova, California) after intracoronary injection of 200 μg of nitroglycerin, at a pullback speed of 0.5 mm/s and a frame speed of 30 frames/s. All pullbacks were analyzed offline at 1-mm longitudinal intervals by an independent core laboratory (Cardialysis BV, Rotterdam, the Netherlands) using commercially available software (QIvus version 2.2, Medis, Leiden, the Netherlands).

The methods of quantitative IVUS have been previously published (1,12). Considering the difficulty in measuring neointima in the biodegraded scaffold at 3 years, to better compare the 2 devices, the

ABBREVIATIONS AND ACRONYMS

BVS = bioresorbable vascular scaffold(s)

DES = drug-eluting stent(s)

IVUS = intravascular ultrasound

LA = lumen area

PCI = percutaneous coronary intervention

VA = vessel area

VH = virtual histology

Dr. van der Schaaf has received institutional research grants from Abbott Vascular. Dr. Baumbach has received research support from Abbott Vascular. Dr. Smits has received research grants from Abbott Vascular and St. Jude Medical; and has received speaker fees from Abbott Vascular and Medinol. Dr. Gershlick has served on the advisory board of and received lecture fees and travel sponsorship from Abbott Vascular. Dr. Ormiston has served on the advisory boards of Boston Scientific and Abbott Vascular. Dr. Egred has received honoraria for proctorship from Abbott, Boston Scientific, Volcano, Biosensors, Vascular Perspectives, Vascular Solutions, and Merrill. Dr. Fajadet has received educational grants from Abbott, Boston Scientific, Medtronic, and Terumo. Dr. Lesiak has received honoraria as a speaker and/or advisory board member from Abbott Vascular, Boston Scientific, AstraZeneca, Biotronik, St. Jude Medical, Terumo, and Volcano. Dr. Windecker has received research grants to his institution from Bracco, Boston Scientific, and Terumo. Dr. Byrne has received lecture fees from B. Braun Melsungen AG, Biotronik, and Boston Scientific; and has received research grants to his institution from Boston Scientific and Heartflow. Dr. Räber has received speaker fees and institutional grants from Abbott, Biotronik, St. Jude Medical, and Sanofi/Regeneron. Dr. van Geuns has received a research grant from Abbott Vascular. Dr. Mintz has received honoraria or grant support from Boston Scientific, Volcano, and ACIST. Dr. Onuma has served as a member of the advisory board for Abbott Vascular; and has received speaker honoraria from Terumo. All other authors have reported that they have no relationships relevant to the contents of this paper to disclose.

Manuscript received March 12, 2017; revised manuscript received April 23, 2017, accepted May 1, 2017.

CENTRAL ILLUSTRATION **Patterns of Vessel Remodeling**

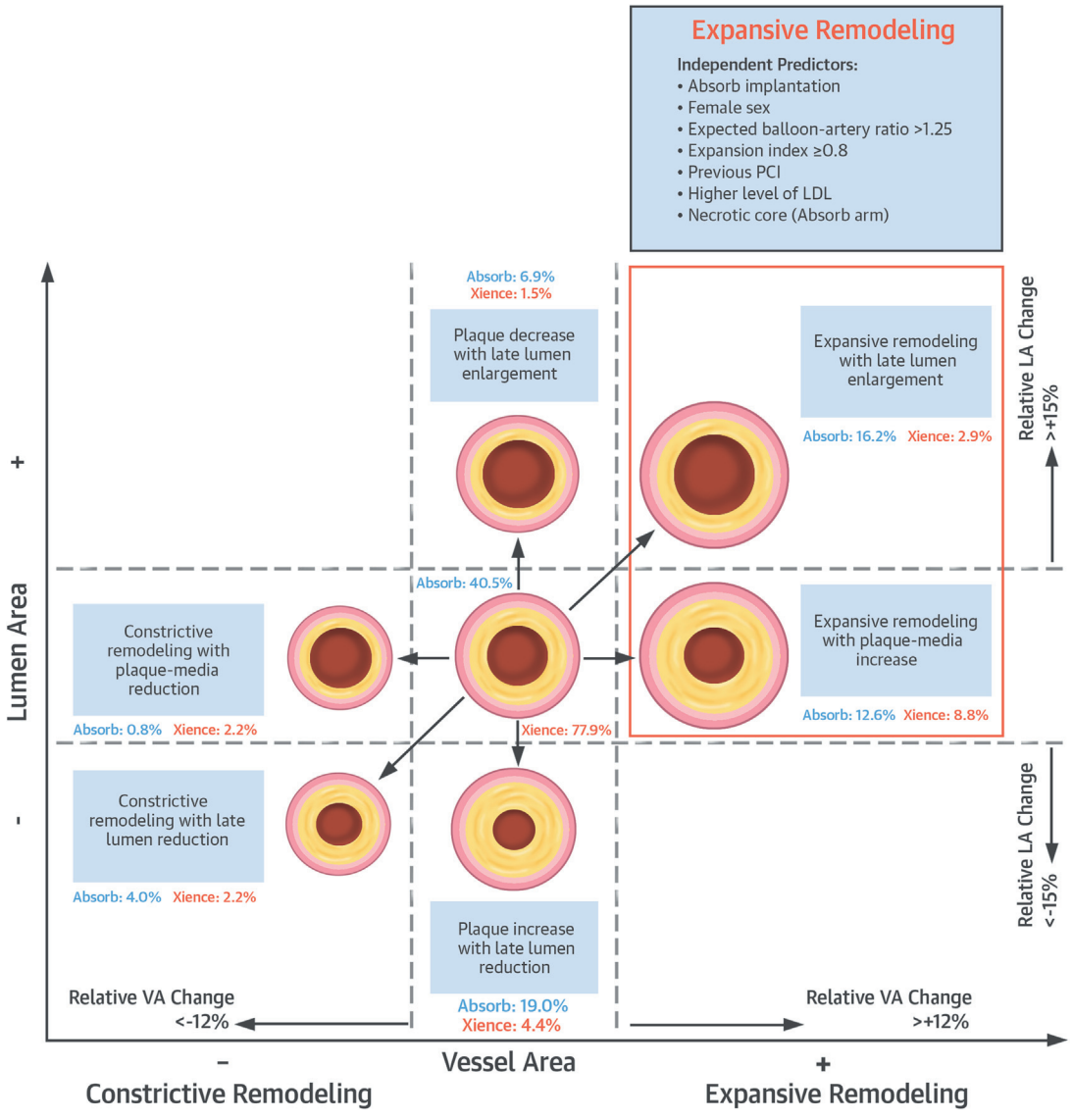

Serruys, P.W. et al. J Am Coll Cardiol. 2017;70(1):60-74.

Relative changes in vessel area (VA) (constrictive remodeling <−12%, expansive remodeling >+12%) and relative changes in lumen area (LA) (lumen reduction <−15%, lumen enlargement >+15%) defined remodeling patterns. No lesions showed constrictive remodeling with LA increase or expansive remodeling with LA decrease. Expansive vessel wall remodeling was more frequent with the bioresorbable vascular scaffold (BVS) than the metallic drug-eluting stent (DES) and could be determined by patient baseline characteristics and periprocedural factors. LDL = low-density lipoprotein; PCI = percutaneous coronary intervention.

intrascaffold-stent neointima was included in the metric "plaque-media = vessel area − lumen area." The reference segments after device implantation were the 5-mm segments proximal and distal to the device. According to a previous study (14), relative range of interobserver reproducibility of measurement for lumen, plaque-media, and vessel cross-sectional areas based on 2 SD of their measurements

FIGURE 1 Study Flow

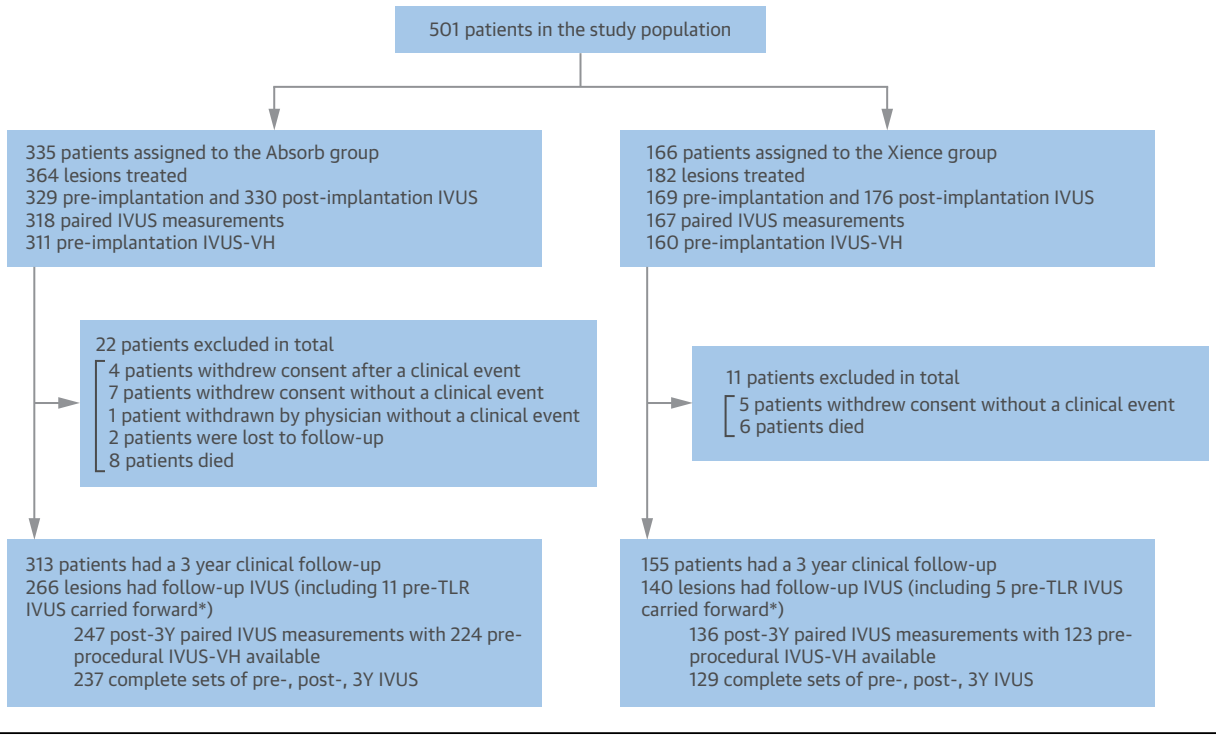

*The results of 18 pre-target lesion revascularization (TLR) intravascular ultrasound (IVUS) were carried forward to 3-year follow-up (3Y) for statistical purposes. VH = virtual histology.

were ±15%, ±22%, and ±12%, respectively. Specifically, expansive remodeling was defined as a relative change in mean VA >+12%, while constrictive remodeling was defined as a relative change in mean VA <−12%. According to these relative values of reproducibility, there were 9 theoretical patterns of vessel-lumen-plaque remodeling based on increase, no change, and decrease in each of the 3 parameters (**Central Illustration**) (3).

The pre-procedure target ("to-be-scaffolded/stented") segments were defined by coregistration with post-procedural IVUS using identical landmarks, such as side branches and calcium locations. Matching was done using dedicated software (IvusOCT-Registration, Division of Image Processing, Leiden, the Netherlands) (15). Pre-procedural IVUS-VH analysis was performed within the target segments. Tissue compositions, derived from pre-procedural IVUS-VH analysis, were expressed in percentages, averaged for multiple plaque-media cross-sectional areas, and related to the different patterns of remodeling at follow-up (16).

Pre-procedural offline or online qualitative comparative analysis (QCA) for the sizing of the device was mandatory. The strategy of device deployment, with or without post-dilation, is described in detail in the protocol as well as the various parameters involved in device deployment (Online Appendix). The maximal diameter of the device/post-dilation balloon throughout the procedure was used for calculation of various balloon-artery ratios, with reference lumen diameter defined either by IVUS using a circular model, as the average of 5-mm segments proximal and distal to the device segment (17), or by QCA using the interpolated method (Online Table 1).

The definitions of expansion index, asymmetry index, eccentricity index, and deployment index are reported in the Online Appendix (15,18-20).

OVERALL SUBSTUDY OBJECTIVES. The primary objective of this study was to elucidate differences in remodeling patterns following BVS or DES implantation. First, differences in mean lumen, vessel, and plaque area changes were to be documented and the

TABLE 1 Baseline Characteristics, Pre-Procedural IVUS Findings, and Procedural Data*

	BVS	DES	p Value
Patient characteristics			
n	233	126	
Age, yrs	61 ± 10	60 ± 10	0.223
Male	172 (73.8)	103 (81.7)	0.09
Current smoking	58 (24.9)	29 (23.0)	0.692
Hypertension requiring medication	148 (63.5)	80 (63.5)	0.996
Dyslipidemia requiring medication	167 (71.7)	90 (71.4)	0.961
Diabetes	50 (21.5)	28 (22.2)	0.867
Unstable angina	41 (17.6)	29 (23.0)	0.216
Prior MI	64 (27.7)	37 (29.4)	0.739
Previous PCI	80 (32.4)	45 (33.1)	0.889
Serum creatinine, μmol/l	80.8 ± 17.6	82.2 ± 19.2	0.484
BMI ≥30 kg/m^2	61 (26.2)	36 (28.6)	0.626
Lesions			
n	247	136	
Lesion location			0.577
Right coronary artery	67 (27.1)	41 (30.1)	
Left anterior descending	112 (45.3)	64 (47.1)	
Left circumflex artery	68 (27.5)	31 (22.8)	
Lesion classification			0.235
A	3 (1.2)	0 (0.0)	
B1	138 (55.9)	71 (52.2)	
B2	103 (41.7)	65 (47.8)	
C	3 (1.2)	0 (0.0)	

Continued on the next page

various patterns of remodeling established. Second, exploratory analysis of remodeling predictors, such as tissue composition analyzed by IVUS-VH and balloon-artery ratio, was performed. Finally, independent predictors for expansive remodeling were determined from multivariate analysis.

STATISTICAL ANALYSIS. Categorical variables are presented as counts and percentages. Continuous variables are presented as mean ± SD or median (interquartile range), as appropriate. A p value <0.05 was considered statistically significant. Categorical variables were compared using chi-square statistics or Fisher exact test. Continuous variables between post-procedure and 3-year follow-up were compared with paired Student *t* test, and those between groups were compared with independent Student *t* test or analysis of variance with application of Bonferroni correction. In case of target lesion revascularization, the IVUS documentation prior to the treatment was carried forward and included in the statistical analysis of the 3-year results. The Pearson correlation coefficient was used to evaluate the strength and direction of the linear relationship between 2 parameters. Receiver-operating characteristic (ROC) analyses were performed to compare diagnostic ability, and Youden index was used to derive the cutoff point. Multivariate logistic regression analysis was performed to find independent determinants of vessel remodeling. The models were constructed using significant variables ($p < 0.05$) of univariate analyses. Statistical analyses were performed with SPSS version 24.0.0.1 (IBM, Armonk, New York).

RESULTS

In the ABSORB II trial, of 546 lesions (n = 501) analyzed at baseline, 247 lesions (n = 233) in the BVS arm and 136 lesions (n = 126) in the DES arm had both post-procedure and 3-year follow-up IVUS images (**Figure 1**). Among lesions with paired post-procedure and 3-year follow-up IVUS, pre-procedural IVUS was available for 237 lesions in the BVS arm and 129 lesions in the DES arm, whereas pre-procedural IVUS-VH was available in 224 and 123 lesions, respectively. Baseline clinical, lesion, and procedural characteristics in patients and lesions with paired post-procedural and 3-year IVUS were well balanced between both arms (**Table 1**). In terms of procedural characteristics, the maximal pressure during device implantation or post-dilation, nominal and expected diameter of post-dilation balloon, and measured diameter of device and post-dilation balloon were significantly higher in the DES arm than in the BVS arm.

The absolute and relative changes in mean LA, plaque-media area, and VA between post-procedure and 3-year follow-up are tabulated in **Table 2** (IVUS parameters post-procedure and at 3-year follow-up are provided in Online Table 2). The relative changes in mean VA, LA, and plaque-media area were significantly different for the 2 arms (**Figure 2**).

The relationship between relative changes in mean LA and mean VA is illustrated in **Figure 3**. To facilitate the understanding of complex relationships among relative changes of mean vessel, lumen, and plaque area, 3-dimensional scatter plots were created (moving images are available in Online Videos 1 and 2). There was a significant positive correlation between the changes in mean VA and mean LA both for the BVS (correlation coefficient [CC]: 0.767; 95% confidence interval [CI]: 0.711 to 0.813; $p < 0.001$; $y = 1.17 \times -6.42$; $R^2 = 0.589$) and for the DES populations (CC: 0.663; 95% CI: 0.557 to 0.747; $p < 0.001$; $y = 0.61 \times -3.65$; $R^2 = 0.440$); however, the distribution in the relative changes in mean VA and mean LA in the BVS arm was more outstretched than the changes observed with DES ($p = 0.0466$; Fisher r-to-z transformation).

Based on the boundaries of interobserver reproducibility of area measurements, we categorized 9 patterns of remodeling per relative changes in mean LA and mean VA (**Central Illustration, Figure 3**). The IVUS parameters post-procedure and at 3 years within each group are provided in Online Table 3.

The lesion subset groups are labeled A through I (**Figure 3**). In the BVS arm, groups B and C showed an increase in mean LA that was beyond interobserver reproducibility. In group B, the increase in mean LA was partially due to a small decrease in plaque-media area and plaque burden. Group C consisted of cases with late lumen enlargement associated with expansive remodeling that exceeded the increase in plaque-media area, resulting in a plaque burden decrease. Group E, with the largest number of observations, consisted of lesions that did not show any change beyond the interobserver reproducibility for VA and LA measurements. Group F displayed an increase in plaque-media, which was largely compensated by an expansive remodeling of the vessel, so that the lumen area showed minor changes, but plaque burden increased. Group G exhibited a decrease in mean LA mainly resulting from constrictive remodeling. Finally, group H comprised lesions with a decrease in mean LA resulting from an increase in mean plaque-media area, not compensated by expansive remodeling.

In the DES arm (**Figure 3**), the large majority of lesions (group E) did not exhibit any change in LA or VA beyond the interobserver reproducibility. The second group in terms of number (group F) was represented by stented lesions that exhibited some degree of VA increase without LA decrease (no intrastent neointimal hyperplasia). Group H was characterized by an LA decrease due to an increase in intrastent neointima not associated with VA increase. The other groups contained fewer than 5 patients.

In both arms, there were no patients with expansive remodeling and a decrease in lumen dimensions or constrictive remodeling with an increase in lumen dimensions (group A or I). In comparing proportions of each remodeling subset in the 2 arms (**Table 3**), expansive remodeling and either lumen enlargement or lumen reduction were more frequent in the BVS arm versus the DES arm, whereas frequency of constrictive remodeling did not differ. Late acquired malapposition was documented in 6 lesions of the BVS arm and was associated with LA increase (Online Table 4). One late acquired malapposition was observed in BVS group E.

Proportions of pre-procedural VH composition (average percentage of each tissue component in plaque-media areas) according to vessel remodeling patterns at follow-up are shown in **Table 4 and Figure 4**. In the BVS arm, there were no significant differences in the proportion of fibrous, fibrofatty tissue and dense calcium between the various vessel remodeling patterns; the proportion with a necrotic core was significantly less in the constrictive remodeling group, but was higher in the expansive

TABLE 1 Continued

	BVS	DES	p Value
Pre-procedural IVUS findings			
Available lesions	237	129	
Mean vessel area, mm^2	11.42 ± 3.43	12.35 ± 3.22	0.01
Mean lumen area, mm^2	4.81 ± 1.41	5.02 ± 1.38	0.158
Mean plaque area, mm^2	6.61 ± 2.49	7.32 ± 2.41	0.008
Mean plaque burden, %	56.98 ± 8.57	58.57 ± 8.49	0.088
Minimum vessel area, mm^2	8.59 ± 3.11	9.47 ± 3.03	0.009
Minimum lumen area, mm^2	2.01 ± 0.71	2.11 ± 0.79	0.269
Reference vessel area, mm^2	11.78 ± 3.84	12.74 ± 3.53	0.016
Procedural details			
Lesions	247	136	
Pre-dilation performed	247 (100.0)	134 (98.5)	0.125
Nominal diameter of pre-dilation balloon, mm	2.61 ± 0.36	2.64 ± 0.36	0.347
Maximal pressure during pre-dilation, atm	12.16 ± 3.00	12.34 ± 3.01	0.574
Nominal diameter of device, mm	3.02 ± 0.31	3.06 ± 0.28	0.191
Length of implanted device, mm	23.60 ± 10.50	23.28 ± 8.79	0.766
Maximal pressure during device implantation, atm	13.26 ± 2.74	13.89 ± 2.62	0.03
Expected device diameter, mm	3.34 ± 0.34	3.28 ± 0.33	0.109
Mean diameter of device balloon measured by QCA, mm	2.71 ± 0.36	2.94 ± 0.33	<0.001
Minimal diameter of device balloon measured by QCA, mm	2.37 ± 0.38	2.63 ± 0.35	<0.001
Post-dilation performed	150 (60.7)	82 (60.3)	0.934
Nominal diameter of post-dilation balloon, mm	3.16 ± 0.33	3.27 ± 0.36	0.016
Maximal pressure during post-dilation, atm	15.26 ± 3.04	16.88 ± 3.39	<0.001
Expected diameter of post-dilation balloon, mm	3.26 ± 0.34	3.39 ± 0.37	0.007
Mean diameter of post-dilation balloon measured by QCA, mm	2.64 ± 0.30	2.99 ± 0.32	<0.001
Minimal diameter of post-dilation balloon measured by QCA, mm	2.41 ± 0.32	2.75 ± 0.32	<0.001
Maximal† mean balloon diameter throughout procedure measured by QCA, mm	2.75 ± 0.33	3.00 ± 0.34	<0.001
Maximal† mean balloon diameter throughout procedure measured by QCA, mm	2.46 ± 0.34	2.73 ± 0.36	<0.001
Post-procedural patient-related factors			
n	233	126	
Mean LDL-C, mmol/l	2.32 ± 0.63	2.29 ± 0.59	0.653

Values are n, mean ± SD, or n (%). *Tabulated values differ from the primary report (13) because the population consisted exclusively of patients and lesions with paired IVUS measurements post-procedure and at 3-year follow-up. †Maximal diameter throughout procedure.

BMI = body mass index; BVS = bioresorbable vascular scaffold; DES = drug-eluting stent; IVUS = intravascular ultrasound; LDL-C = low-density lipoprotein cholesterol; MI = myocardial infarction; PCI = percutaneous coronary intervention; QCA = qualitative comparative analysis.

TABLE 2 IVUS Parameters

	BVS (n = 247)	DES (n = 136)	p Value
Absolute change			
Mean VA, mm^2	0.75 ± 1.66	0.31 ± 1.29	0.004
Mean LA, mm^2	0.07 ± 1.20	−0.15 ± 0.70	0.02
Mean plaque area, mm^2	0.67 ± 1.01	0.46 ± 1.01	0.047
Mean plaque burden, %	2.68 ± 5.58	2.29 ± 4.24	0.451
Relative change			
Mean VA, %	6.7 ± 12.6	2.9 ± 11.5	0.003
Mean LA, %	1.4 ± 19.1	−1.9 ± 10.5	0.031
Mean plaque area, %	12.4 ± 16.0	8.5 ± 18.9	0.042
Mean plaque burden, %	5.6 ± 11.2	5.0 ± 8.9	0.572

Values are mean ± SD.
LA = lumen area; VA = vessel area; other abbreviations as in Table 1.

remodeling group than in the group without vessel remodeling. In the DES arm, there were no significant differences in IVUS-VH composition for each remodeling group. ROC analysis of the proportion of necrotic core that predicted expansive remodeling in the BVS cases showed an area under the curve of 0.63 (95% CI: 0.55 to 0.71; p = 0.004) with a cutoff value of 16.7% (sensitivity 61.0%, specificity 61.8%). ROC analysis performed in the DES group did not show significance (p = 0.255).

The nominal, expected, or measured value of the maximal balloon diameter and balloon-artery ratios for the 3 categories of vessel remodeling (constrictive, no change in VA, expansive) are shown in Table 5 and Figure 5. Overall, the balloon diameters, either nominal or expected or measured by QCA (mean or minimal), failed to show any relationships with the development of constrictive or expansive remodeling in either group. However, increased balloon-artery ratios were associated with expansive remodeling in the BVS arm, in particular when nominal and expected balloon-artery ratios were used; only the QCA-measured balloon-artery ratio was associated with expansive remodeling in the DES arm.

The ROC analysis of expected balloon-artery ratio, among other balloon-artery ratios, showed the largest area under the curve (0.69; 95% CI: 0.61 to 0.77; p < 0.001) with a cutoff point of 1.25 (sensitivity

FIGURE 2 Mean Area Changes

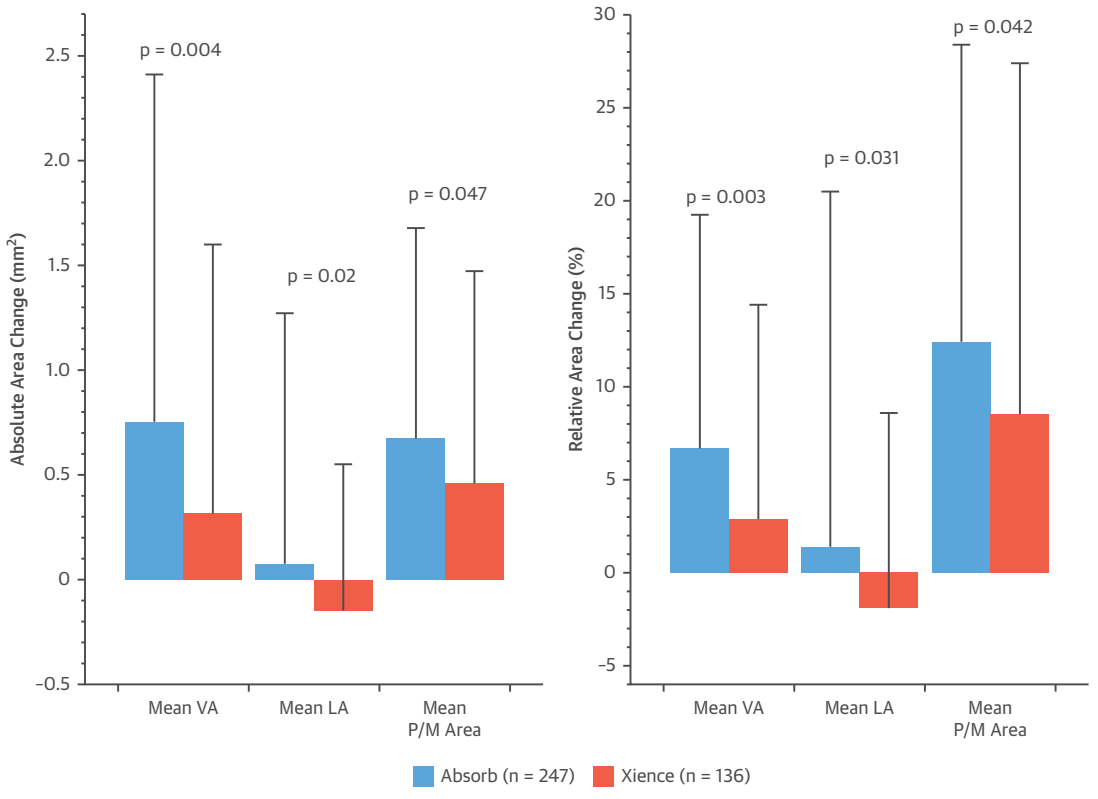

Significant absolute and relative area changes on IVUS were seen between post-procedure and 3Y. LA = lumen area; P/M = plaque-media; VA = vessel area; other abbreviations as in Figure 1.

FIGURE 3 **Relationship Between Relative Change in Mean VA and LA**

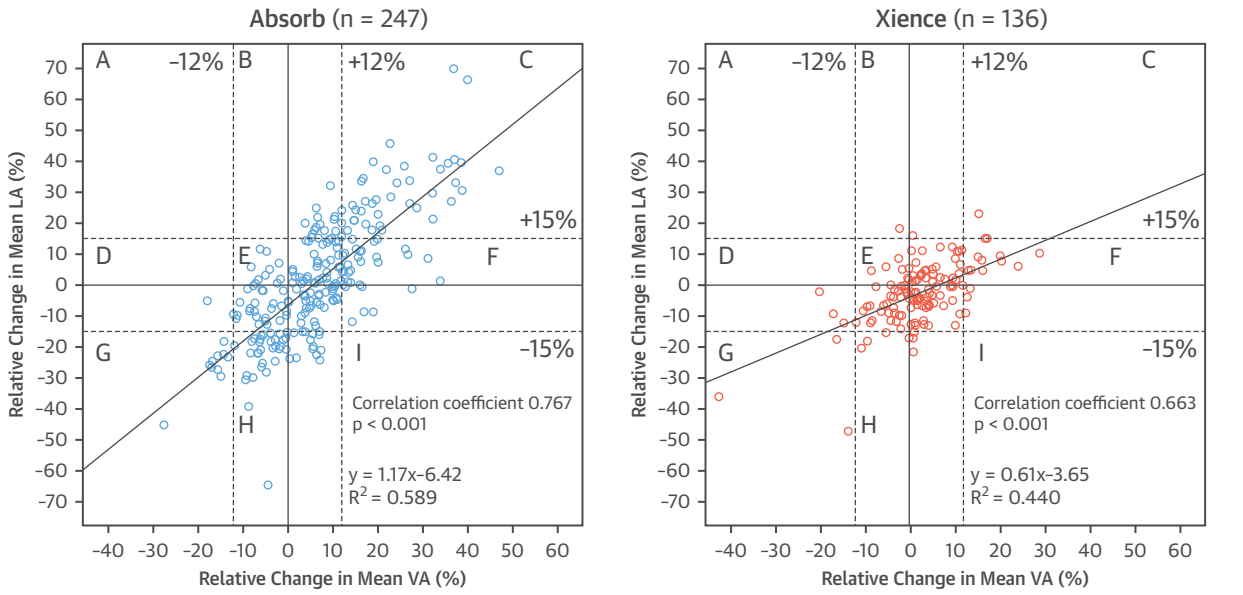

	Absorb (n = 247)	Xience (n = 136)	P value*
A. Constrictive remodeling with late lumen enlargement	0 (0)	0 (0)	-
B. Plaque media decrease with late lumen enlargement	17 (6.9)	2 (1.5)	0.020
C. Expansive remodeling with late lumen enlargement	40 (16.2)	4 (2.9)	<0.001
D. Constrictive remodeling with plaque/media reduction	2 (0.8)	3 (2.2)	0.352
E. Within the reproducibility of the measurement	100 (40.5)	106 (77.9)	<0.001
F. Expansive remodeling with plaque/media increase	31 (12.6)	12 (8.8)	0.269
G. Constrictive remodeling with late lumen reduction	10 (4.0)	3 (2.2)	0.395
H. Plaque/media increase with late lumen reduction	47 (19)	6 (4.4)	<.0001
I. Expansive remodeling with late lumen reduction	0 (0)	0 (0)	-

A total of 9 patterns of remodeling were characterized; **reference lines** indicate ±12% relative change in mean VA and ±15% relative change in mean LA (boundaries for interobserver reproducibility). Data are counts (%). Absolute values in each group are tabulated in Online Table 3. To facilitate the understanding of complex relationships among relative changes of mean vessel, lumen, and plaque area, 3-dimensional scatter plots were created (Online Videos 1 and 2). *p value for chi-square test. Abbreviations as in **Figure 2**.

61.0%, specificity 75.3%) for prediction of expansive remodeling in the BVS arm. ROC analysis of expected balloon-artery ratio performed in the DES group did not show significance (p = 0.174).

Predictors for expansive remodeling (n = 87 lesions, 22.7%) were analyzed by multivariate logistic regression analysis, whereas predictors for constrictive remodeling were not investigated due to the limited number of lesions with constrictive remodeling (n = 18 lesions, 4.7%). Online Table 5 shows the result of univariate analysis for predictors of expansive remodeling. Subsequent multivariate analysis (**Table 6**) identified that BVS implantation, female sex, balloon-artery ratio by maximal expected diameter of balloon throughout procedure >1.25, expansion index ≥0.8, previous PCI, and higher mean LDL-C over 3 years were independent predictors for expansive remodeling. When the multivariate model was applied to the BVS population only, pre-procedural proportion of necrotic core >16.7% became significant. The multivariate analysis of the DES arm is not formally reported due to the small number of lesions showing expansive remodeling (16 lesions, 11.8%). However, the effect of the device type (p value for interaction) was not significantly different for each independent determinant of expansive

TABLE 3 Difference in Proportions of Mean VA and LA Changes*

	BVS (n = 247)	DES (n = 136)	p Value†
Expansive remodeling (C, F, I)	71 (28.7)	16 (11.8)	<0.001
Constrictive remodeling (A, D, G)	12 (4.9)	6 (4.4)	0.843
Lumen enlargement (A, B, C)	57 (23.1)	6 (4.4)	<0.001
Lumen reduction (G, H, I)	57 (23.1)	9 (6.6)	<0.001
No significant change in either VA or LA (E)	100 (40.5)	106 (77.9)	<0.001

Values are n (%). *Letters correspond to subset designations in Figure 3. †Chi-square test.
Abbreviations as in Tables 1 and 2.

remodeling identified by the multivariate analysis, despite some trends that might become significant in a larger sample size population (Figure 6).

DISCUSSION

In this study, the main findings were: 1) lesions treated with the BVS exhibited a larger increase in mean VA than DES-treated lesions; 2) scaffold implantation, female sex, the maximal expected balloon-artery ratio >1.25, expansion index ≥0.8, previous PCI, and higher mean level of LDL-C (average over 3 years) were independent factors predicting expansive remodeling; and 3) pre-procedural greater proportion of necrotic core (threshold of >16.7% in mean plaque area) was also an independent predictor for expansive remodeling, especially in the BVS arm.

At a single time point in a post-mortem study, Glagov et al. (2) reported that the LA was not decreased in relation to any plaque burden increase for values between 0% and 40%, but beyond that threshold, the compensatory expansive remodeling was no longer operational. In fact, very few lesions investigated in the present study had plaque burden <40% (Online Table 2); however, the relationship between LA and plaque burden >40% was consistent with Glagov's theorem (Figure 7). In our serial analysis, taking into

FIGURE 4 Plaque Composition

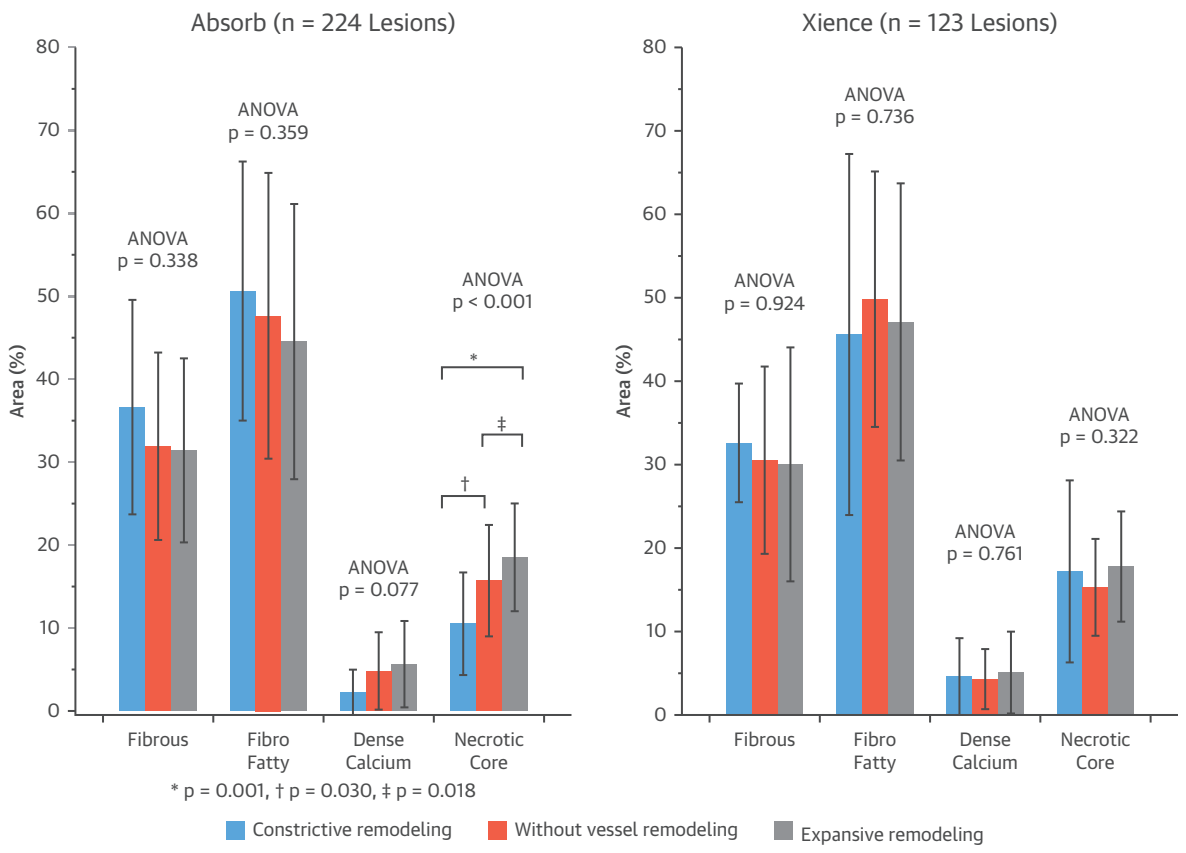

Pre-procedural plaque composition as analyzed by intravascular ultrasound-virtual histology is seen in 3 categories of vessel remodeling. *p = 0.001. †p = 0.030. ‡p = 0.018. ANOVA = analysis of variance.

account the measurement variability of the plaque burden metrics, true plaque burden regression could not be documented in both arms, whereas plaque burden increase was observed in 12.1% in the BVS arm and 4.5% in the DES arm. However, the slope of the relationship between plaque burden and LA was 2-fold steeper in the scaffold arm (0.16) when compared to the DES arm (0.08), exemplifying the remodeling capability of the scaffolds.

VASCULAR RESPONSE AFTER INTERVENTION AND FUNCTION OF SCAFFOLDING. In the era of balloon angioplasty, restenosis was caused mainly by constrictive remodeling (4). In a study using serial IVUS after angioplasty or directional coronary atherectomy, expansive remodeling was observed up to 1 month, but luminal reduction prevailed from 1 to 6 months, mainly due to negative remodeling (5,6). Between 6 months and 5 years, most patients have luminal enlargement after balloon angioplasty (7).

Bare-metal stents were found to prevent constrictive remodeling, but generated intrastent neointimal hyperplasia resulting in some cases of in-stent restenosis (8). Antiproliferative drug-eluting metallic stents are effective to reduce intrastent neointimal hyperplasia (21). With

TABLE 4 Plaque Composition of Mean Plaque Cross-Sectional Area

	Constrictive Remodeling	Without Vessel Remodeling	Expansive Remodeling	p Value*
BVS				
n	12	153	59	
Fibrous tissue, %	36.6 ± 12.9	31.9 ± 11.3	31.4 ± 11.1	0.338
Fibrofatty, %	50.6 ± 15.6	47.6 ± 17.2	44.5 ± 16.6	0.359
Dense calcium, %	2.2 ± 2.7	4.8 ± 4.7	5.6 ± 5.2	0.077
Necrotic core, %	10.5 ± 6.2	15.7 ± 6.7	18.5 ± 6.5	<0.001
DES				
n	4	105	14	
Fibrous tissue, %	32.6 ± 7.1	30.5 ± 11.2	30 ± 14	0.924
Fibrofatty, %	45.6 ± 21.6	49.8 ± 15.3	47.1 ± 16.6	0.736
Dense calcium, %	4.6 ± 4.6	4.3 ± 3.6	5.1 ± 4.9	0.761
Necrotic core, %	17.2 ± 10.9	15.3 ± 5.8	17.8 ± 6.6	0.322

Values are n or mean ± SD. *p value for analysis of variance (ANOVA).
Abbreviations as in Table 1.

TABLE 5 Balloon Diameters and Balloon-Artery Ratios

	Cases With Parameter Available	Constrictive Remodeling	No Change in VA	Expansive Remodeling	p Value*
BVS (n = 247)					
Maximal nominal balloon diameter, mm	247	3.08 ± 0.27	3.11 ± 0.33	3.10 ± 0.32	0.951
Maximal expected balloon diameter, mm	247	3.43 ± 0.36	3.36 ± 0.33	3.41 ± 0.34	0.504
Maximal mean balloon diameter measured by QCA, mm	240	2.84 ± 0.26	2.75 ± 0.35	2.74 ± 0.32	0.626
Maximal minimal balloon diameter measured by QCA, mm	240	2.59 ± 0.25	2.45 ± 0.35	2.45 ± 0.35	0.381
Balloon-artery ratio by maximal nominal balloon diameter	209	0.99 ± 0.10	1.08 ± 0.14	1.17 ± 0.17	<0.001
Balloon-artery ratio by maximal expected balloon diameter	209	1.09 ± 0.10	1.17 ± 0.18	1.29 ± 0.20	<0.001
Balloon-artery ratio by maximal mean balloon diameter measured by QCA	239	1.02 ± 0.14	1.06 ± 0.13	1.08 ± 0.10	0.313
Balloon-artery ratio by maximal MLD of balloon measured by QCA	239	0.93 ± 0.12	0.94 ± 0.13	0.96 ± 0.11	0.638
DES (n = 136)					
Maximal nominal balloon diameter, mm	136	3.04 ± 0.19	3.19 ± 0.34	3.05 ± 0.29	0.194
Maximal expected balloon diameter, mm	136	3.09 ± 0.32	3.28 ± 0.35	3.27 ± 0.40	0.423
Maximal mean balloon diameter measured by QCA, mm	136	2.77 ± 0.20	3.02 ± 0.34	2.94 ± 0.37	0.158
Maximal minimal balloon diameter measured by QCA, mm	136	2.52 ± 0.20	2.74 ± 0.36	2.70 ± 0.35	0.315
Balloon-artery ratio by maximal nominal balloon diameter	116	1.10 ± 0.06	1.10 ± 0.15	1.13 ± 0.14	0.818
Balloon-artery ratio by maximal expected balloon diameter	116	1.11 ± 0.12	1.13 ± 0.18	1.21 ± 0.23	0.326
Balloon-artery ratio by maximal mean balloon diameter measured by QCA	134	1.09 ± 0.12	1.15 ± 0.14	1.24 ± 0.16	0.041
Balloon-artery ratio by maximal MLD of balloon measured by QCA	134	1.00 ± 0.11	1.04 ± 0.13	1.13 ± 0.14	0.027

Values are n or mean ± SD. *p value for ANOVA.
MLD = minimal lumen diameter; QCA = quantitative coronary angiography; other abbreviations as in Tables 1, 2, and 4.

FIGURE 5 Balloon-Artery Ratios

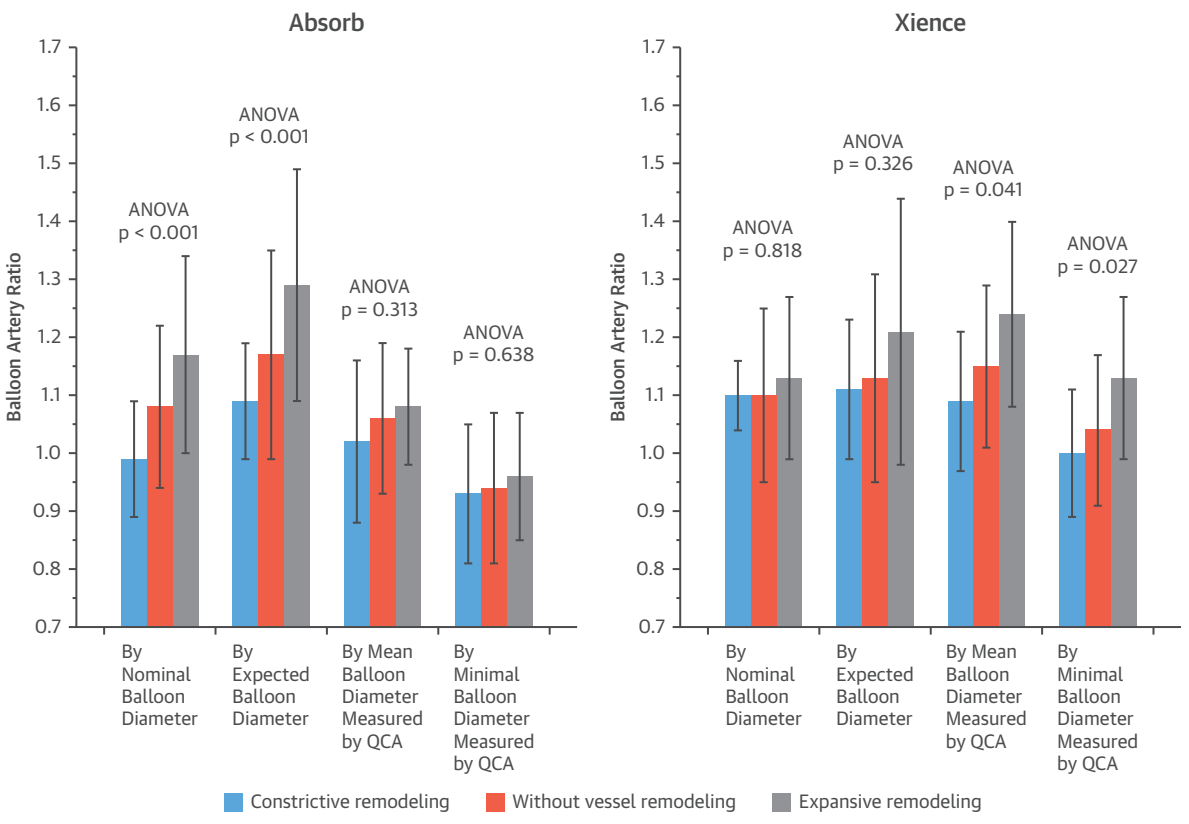

Balloon-artery ratios are shown for 3 categories of vessel remodeling. ANOVA = analysis of variance; QCA = quantitative coronary angiography.

early-generation DES, positive remodeling leading to late acquired malapposition could occur, whereas this phenomenon is almost absent in newer-generation DES (22).

Drug-eluting bioresorbable scaffolds prevent constrictive remodeling in the first 6 months following implantation, but after the loss of their mechanical integrity, they allow expansive remodeling modulated by predictors described in the following text (23-25).

In contrast to the current study, the mean LA observed by optical coherent tomography in ABSORB cohort B at 3 years was stable after the initial decrease at 6 months (10). However, due to the shorter penetration depth, optical coherent tomography could not evaluate VA and remodeling as IVUS was able to in this study.

PREDICTORS FOR EXPANSIVE REMODELING. In the present study, BVS implantation was an independent predictor for expansive remodeling. In previous observational studies, it has been documented that the mechanical support of scaffolds is lost 6 to 12 months after implantation (23) and that vessel and scaffold can potentially enlarge subsequently. In the preclinical study by Otsuka et al. (26), BVS implantation had a greater inflammation score than the metallic stents studied here; the scaffolds exhibited expansive remodeling 12 months after implantation, which was paralleled by LA enlargement, whereas metallic stents showed minimal change in vessel size. Considering the interaction between polymer degradation and inflammatory response (27), polymer absorption may promote inflammation and consecutive expansive remodeling after BVS implantation. However, the resorption of lactic acid is not a sole driver, if at all. Loss in scaffold structures (late structural discontinuity) and recovery of pulsatility might also contribute to remodeling mediated by inflammation (28,29) and may play a major role in late lumen enlargement and vessel remodeling. Besides the

FIGURE 6 **Interaction Analysis Between Remodeling Predictors and Device Type**

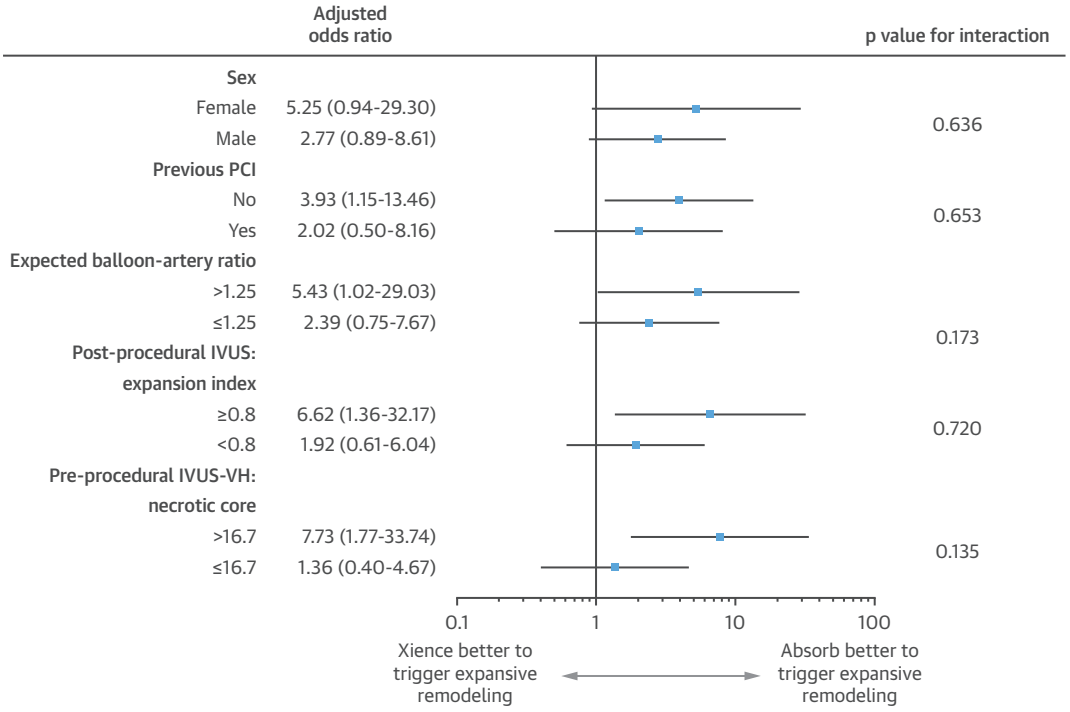

There was no significant difference by device type for each determinant of expansive remodeling. PCI = percutaneous coronary intervention; other abbreviations as in Figure 1.

inflammatory response, another determinant of remodeling might be shear stress, whose influence is currently being investigated (30).

Female sex was also an independent predictor for expansive remodeling in the current study. In an IVUS substudy of the WISE (Women's Ischemia Syndrome Evaluation) study, there was a high prevalence of atherosclerosis with positive remodeling and preserved lumen size (31). Considering that estrogen has anti-inflammatory effects, the pro-inflammatory status after menopause might promote expansive remodeling (32).

Among the balloon-artery ratios investigated, the ratio calculated with the expected balloon diameter

TABLE 6 **Multivariate Analysis: Predictors of Expansive Remodeling**

	Overall			BVS		
	Adjusted OR	95% CI	p Value	Adjusted OR	95% CI	p Value
Absorb implantation	2.85	1.16-6.96	0.022	NA		
Female	2.84	1.35-5.96	0.006	3.25	1.35-7.81	0.008
Balloon-artery ratio by maximal expected diameter of balloon throughout procedure >1.25	2.45	1.11-5.41	0.026	3.17	1.23-8.14	0.017
Post-procedural IVUS: expansion index ≥0.80	2.44	1.11-5.36	0.026	3.91	1.49-10.22	0.005
Previous PCI	2.13	1.04-4.34	0.038	2.09	0.90-4.86	0.088
Mean LDL-C over 3 yrs, per mmol/l	2.10	1.20-3.65	0.009	2.67	1.38-5.17	0.004
Pre-procedural IVUS-VH: necrotic core >16.7%	1.64	0.81-3.31	0.166	2.5	1.08-5.79	0.033
Post-procedural IVUS: asymmetry index >0.30	1.49	0.64-3.44	0.352	1.65	0.60-4.52	0.334
Post-procedural IVUS: eccentricity index <0.70	1.21	0.49-2.99	0.686	0.95	0.35-2.57	0.922
Pre-procedural IVUS: mean LA, per mm^2	0.97	0.63-1.50	0.896	0.91	0.54-1.55	0.73
Pre-procedural IVUS: mean VA, per mm^2	0.90	0.75-1.08	0.236	1.00	0.81-1.23	0.966

CI = confidence interval; NA = not available; OR = odds ratio; VH = virtual histology; other abbreviations as in Tables 1 and 2.

FIGURE 7 Relation Between Plaque Burden Change and Lumen Area

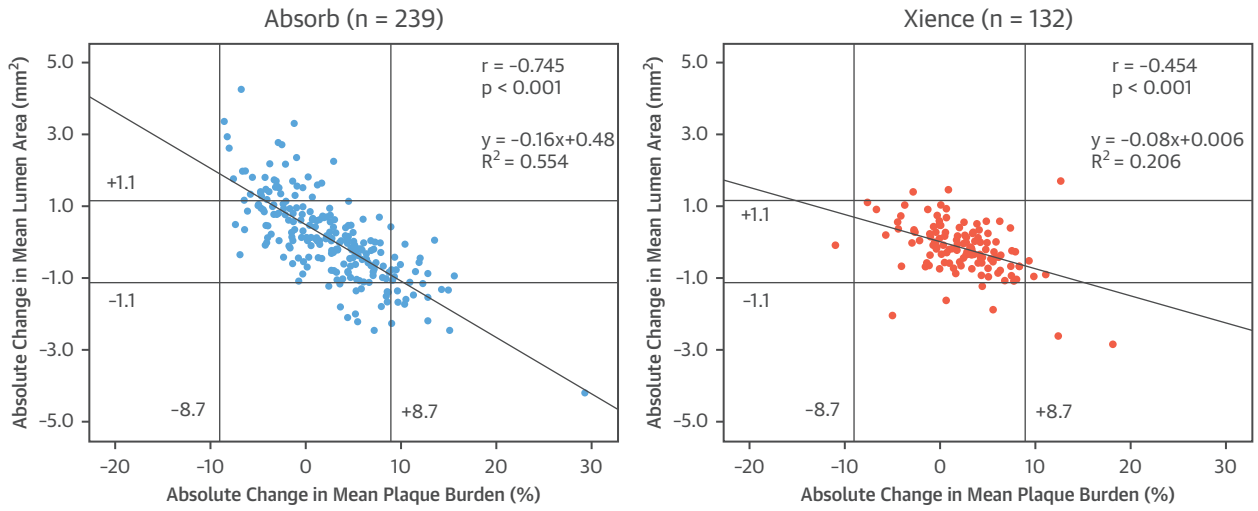

Lesions with mean plaque burden ≥40% in both post-procedure and at 3-year follow-up were plotted. Lines representing reproducibility range of lumen area (−1.1 ∼ +1.1 mm^2) and plaque burden (−8.7 ∼ +8.7%) are superimposed (14). In plotting lesions with mean plaque burden ≥40% post-procedure and at 3-year follow-up, a steeper slope with BVS denoted scaffold remodeling capability. *r = Pearson's correlation efficient.

had the best predictive value, probably because the parameter also incorporates the inflation pressure. The expected balloon diameter concept has been appropriately criticized because this parameter was evaluated in vitro, in the absence of any constraining force, such as a calcified or fibrotic wall; however, in this study, the statistical analysis based on a sensitivity-specificity indicator led us to discover that an expected balloon-artery ratio >1.25 was an independent procedural parameter predicting an expansive remodeling process in a large-scale clinical study. A high balloon-artery ratio resulted in vascular injury, which has been reported to induce expansive remodeling (33) through macrophage infiltration and matrix metalloproteinase increase (34). Also, the relationship between expansion index and vessel remodeling must rely on the same pathophysiological principle.

Higher LDL-C and necrotic core have previously been reported as predictors of expansive remodeling (35–37). Higher LDL-C level can increase necrotic core, oxidize lipid pool in vessel walls, and induce inflammatory responses involving metalloproteinases that promote vessel enlargement (38,39). The concomitant presence of a pre-existing inflammatory process (necrotic core) and the inflammatory process specifically related to the bioabsorption of the polymer may lead to longer and stronger inflammation-inducing expansive remodeling (26,40).

STUDY LIMITATIONS. The major limitation of this study is the intravascular character of the investigation; whenever the IVUS catheter did not or could not cross the scaffolded or stented area, IVUS data for serial assessment were not available, which could potentially bias the serial analysis of wall dynamics. Of 32 patients who had repeat target lesion revascularization, 18 had intravascular imaging before repeat treatment of their target lesion, whereas the remaining 14 were not assessed. The expected balloon-artery ratio was only available in 325 of 383 lesions (84.9%) due to the lack of IVUS-measured reference lumen diameter. The univariate predictive value of necrotic core for positive remodeling was weak according to the low area under the curve. However, the identified threshold emerged as an independent predictor in the multivariate analysis in conjunction with other parameters. Multivariate analyses for constrictive remodeling could not be performed due to the limited number of lesions. At the present stage, the clinical significance of (expansive) remodeling with the BVS studied here is unclear due to the small number of patients enrolled as well as the small number of events reported.

CONCLUSIONS

In the ABSORB II trial, BVS use showed frequent dynamic vessel remodeling with larger increase in mean lumen and vessel area than the comparator DES. This vessel remodeling was determined by patient baseline characteristics and periprocedural factors including balloon-artery ratio and expansion index. The clinical effect of this observed lumen and vessel remodeling requires investigation in further large clinical studies.

ADDRESS FOR CORRESPONDENCE: Prof. Patrick W. Serruys, ThoraxCenter, Erasmus Medical Center, Westblaak 98, Entrance B, 6th Floor, P.O. Box 2125, 3000 CC Rotterdam, the Netherlands. E-mail: patrick.w.j.c.serruys@gmail.com.

PERSPECTIVES

COMPETENCY IN PATIENT CARE AND PROCEDURAL SKILLS:

Coronary lesions treated with bioresorbable scaffolds more frequently exhibit expansive remodeling than those treated with metallic stents. In addition, patient characteristics and procedural factors such as balloon-artery ratio and expansion index also influence vessel remodeling.

TRANSLATIONAL OUTLOOK: Additional research is needed to elucidate the relationship between dynamic vessel remodeling and clinical outcomes in patients undergoing percutaneous revascularization with these devices.

REFERENCES

1. Mintz GS, Nissen SE, Anderson WD, et al. American College of Cardiology clinical expert consensus document on standards for acquisition, measurement and reporting of intravascular ultrasound studies (IVUS): a report of the American College of Cardiology Task Force on Clinical Expert Consensus Documents. J Am Coll Cardiol 2001;37:1478–92.

2. Glagov S, Weisenberg E, Zarins CK, Stankunavicius R, Kolettis GJ. Compensatory enlargement of human atherosclerotic coronary arteries. N Engl J Med 1987;316:1371–5.

3. Van Mieghem CA, Bruining N, Schaar JA, et al. Rationale and methods of the integrated biomarker and imaging study (IBIS): combining invasive and non-invasive imaging with biomarkers to detect subclinical atherosclerosis and assess coronary lesion biology. Int J Cardiovasc Imaging 2005;21:425–41.

4. Mintz GS, Popma JJ, Pichard AD, et al. Arterial remodeling after coronary angioplasty: a serial intravascular ultrasound study. Circulation 1996;94:35–43.

5. Kimura T, Kaburagi S, Tamura T, et al. Remodeling of human coronary arteries undergoing coronary angioplasty or atherectomy. Circulation 1997;96:475–83.

6. Mintz GS, Kimura T, Nobuyoshi M, Leon MB. Intravascular ultrasound assessment of the relation between early and late changes in arterial area and neointimal hyperplasia after percutaneous transluminal coronary angioplasty and directional coronary atherectomy. Am J Cardiol 1999;83:1518–23.

7. Ormiston JA, Stewart FM, Roche AH, Webber BJ, Whitlock RM, Webster MW. Late regression of the dilated site after coronary angioplasty: a 5-year quantitative angiographic study. Circulation 1997;96:468–74.

8. Hoffmann R, Mintz GS, Dussaillant GR, et al. Patterns and mechanisms of in-stent restenosis. A serial intravascular ultrasound study. Circulation 1996;94:1247–54.

9. Serruys PW, Garcia-Garcia HM, Onuma Y. From metallic cages to transient bioresorbable scaffolds: change in paradigm of coronary revascularization in the upcoming decade? Eur Heart J 2012;33:16–25b.

10. Serruys PW, Onuma Y, Garcia-Garcia HM, et al. Dynamics of vessel wall changes following the implantation of the absorb everolimus-eluting bioresorbable vascular scaffold: a multi-imaging modality study at 6, 12, 24 and 36 months. EuroIntervention 2014;9:1271–84.

11. Serruys PW, Ormiston JA, Onuma Y, et al. A bioabsorbable everolimus-eluting coronary stent system (ABSORB): 2-year outcomes and results from multiple imaging methods. Lancet 2009;373:897–910.

12. Diletti R, Serruys PW, Farooq V, et al. ABSORB II randomized controlled trial: a clinical evaluation to compare the safety, efficacy, and performance of the Absorb everolimus-eluting bioresorbable vascular scaffold system against the XIENCE everolimus-eluting coronary stent system in the treatment of subjects with ischemic heart disease caused by de novo native coronary artery lesions: rationale and study design. Am Heart J 2012;164:654–63.

13. Serruys PW, Chevalier B, Sotomi Y, et al. Comparison of an everolimus-eluting bioresorbable scaffold with an everolimus-eluting metallic stent for the treatment of coronary artery stenosis (ABSORB II): a 3 year, randomised, controlled, single-blind, multicentre clinical trial. Lancet 2016;388:2479–91.

14. Muramatsu T, Garcia-Garcia HM, Brugaletta S, et al. Reproducibility of intravascular ultrasound radiofrequency data analysis (virtual histology) with a 45-MHz rotational imaging catheter in ex vivo human coronary arteries. J Cardiol 2015;65:134–42.

15. Suwannasom P, Sotomi Y, Ishibashi Y, et al. The impact of post-procedural asymmetry, expansion, and eccentricity of bioresorbable everolimus-eluting scaffold and metallic everolimus-eluting stent on clinical outcomes in the ABSORB II trial. J Am Coll Cardiol Intv 2016;9:1231–42.

16. Garcia-Garcia HM, Costa MA, Serruys PW. Imaging of coronary atherosclerosis: intravascular ultrasound. Eur Heart J 2010;31:2456–69.

17. Tateishi H, Suwannasom P, Sotomi Y, et al. Edge vascular response after resorption of the everolimus-eluting bioresorbable vascular scaffold- a 5-year serial optical coherence tomography study. Circ J 2016;80:1131–41.

18. de Jaegere P, Mudra H, Figulla H, et al. Intravascular ultrasound-guided optimized stent deployment. Immediate and 6 months clinical and angiographic results from the Multicenter Ultrasound Stenting in Coronaries Study (MUSIC Study). Eur Heart J 1998;19:1214–23.

19. von Birgelen C, Gil R, Ruygrok P, et al. Optimized expansion of the Wallstent compared with the Palmaz-Schatz stent: on-line observations with two- and three-dimensional intracoronary ultrasound after angiographic guidance. Am Heart J 1996;131:1067–75.

20. Sotomi Y, Suwannasom P, Serruys PW, Onuma Y. Possible mechanical causes of scaffold thrombosis: insights from case reports with intracoronary imaging. EuroIntervention 2017;12:1747–56.

21. Rensing BJ, Vos J, Smits PC, et al. Coronary restenosis elimination with a sirolimus eluting stent: first European human experience with 6-month angiographic and intravascular ultrasonic follow-up. Eur Heart J 2001;22:2125–30.

22. Toledano Delgado FJ, Alvarez-Ossorio MP, de Lezo Cruz-Conde JS, et al. Optical coherence tomography evaluation of late strut coverage patterns between first-generation drug-eluting stents and everolimus-eluting stent. Catheter Cardiovasc Interv 2014;84:720–6.

23. Serruys PW, Onuma Y, Ormiston JA, et al. Evaluation of the second generation of a bioresorbable everolimus drug-eluting vascular scaffold for treatment of de novo coronary artery stenosis: six-month clinical and imaging outcomes. Circulation 2010;122:2301–12.

24. Brugaletta S, Gomez-Lara J, Serruys PW, et al. Serial in vivo intravascular ultrasound-based

echogenicity changes of everolimus-eluting bioresorbable vascular scaffold during the first 12 months after implantation insights from the ABSORB B trial. J Am Coll Cardiol Intv 2011;4:1281–9.

25. Serruys PW, Ormiston J, van Geuns RJ, et al. A polylactide bioresorbable scaffold eluting everolimus for treatment of coronary stenosis: 5-year follow-up. J Am Coll Cardiol 2016;67:766–76.

26. Otsuka F, Pacheco E, Perkins LE, et al. Long--term safety of an everolimus-eluting bioresorbable vascular scaffold and the cobalt-chromium XIENCE V stent in a porcine coronary artery model. Circ Cardiovasc Interv 2014;7:330–42.

27. Shive MS, Anderson JM. Biodegradation and biocompatibility of PLA and PLGA microspheres. Adv Drug Deliv Rev 1997;28:5–24.

28. Nakatani S, Ishibashi Y, Sotomi Y, et al. Bioresorption and vessel wall integration of a fully bioresorbable polymeric everolimus-eluting scaffold: optical coherence tomography, intravascular ultrasound, and histological study in a porcine model with 4-year follow-up. J Am Coll Cardiol Intv 2016;9:838–51.

29. Onuma Y, Serruys PW, Muramatsu T, et al. Incidence and imaging outcomes of acute scaffold disruption and late structural discontinuity after implantation of the absorb Everolimus-Eluting fully bioresorbable vascular scaffold: optical coherence tomography assessment in the ABSORB cohort B trial (A Clinical Evaluation of the Bioabsorbable Everolimus Eluting Coronary Stent System in the Treatment of Patients With De Novo Native Coronary Artery Lesions). J Am Coll Cardiol Intv 2014;7:1400–11.

30. Serruys PW, Onuma Y. Dmax for sizing, PSP-1, PSP-2, PSP-3 or OCT guidance: interventionalist's jargon or indispensable implantation techniques for short- and long-term outcomes of Absorb BRS? EuroIntervention 2017;12:2047–56.

31. Khuddus MA, Pepine CJ, Handberg EM, et al. An intravascular ultrasound analysis in women experiencing chest pain in the absence of obstructive coronary artery disease: a substudy from the National Heart, Lung and Blood Institute–sponsored Women's Ischemia Syndrome Evaluation (WISE). J Interv Cardiol 2010;23:511–9.

32. Burke AP, Farb A, Malcom G, Virmani R. Effect of menopause on plaque morphologic characteristics in coronary atherosclerosis. Am Heart J 2001;141:S58–62.

33. Okura H, Shimodozono S, Hayase M, Bonneau HN, Yock PG, Fitzgerald PJ. Impact of deep vessel wall injury and vessel stretching on subsequent arterial remodeling after balloon angioplasty: a serial intravascular ultrasound study. Am Heart J 2002;144:323–8.

34. Yamashita A, Shoji K, Tsuruda T, et al. Medial and adventitial macrophages are associated with expansive atherosclerotic remodeling in rabbit femoral artery. Histol Histopathol 2008;23:127–36.

35. Tauth J, Pinnow E, Sullebarger JT, et al. Predictors of coronary arterial remodeling patterns in patients with myocardial ischemia. Am J Cardiol 1997;80:1352–5.

36. Hibi K, Ward MR, Honda Y, et al. Impact of different definitions on the interpretation of coronary remodeling determined by intravascular ultrasound. Catheter Cardiovasc Interv 2005;65:233–9.

37. Kaple RK, Maehara A, Sano K, et al. The axial distribution of lesion-site atherosclerotic plaque components: an in vivo volumetric intravascular ultrasound radio-frequency analysis of lumen stenosis, necrotic core and vessel remodeling. Ultrasound Med Biol 2009;35:550–7.

38. Holvoet P, Theilmeier G, Shivalkar B, Flameng W, Collen D. LDL hypercholesterolemia is associated with accumulation of oxidized LDL, atherosclerotic plaque growth, and compensatory vessel enlargement in coronary arteries of miniature pigs. Arterioscler Thromb Vasc Biol 1998;18:415–22.

39. Schoenhagen P, Vince DG, Ziada KM, et al. Relation of matrix-metalloproteinase 3 found in coronary lesion samples retrieved by directional coronary atherectomy to intravascular ultrasound observations on coronary remodeling. Am J Cardiol 2002;89:1354–9.

40. Seimon T, Tabas I. Mechanisms and consequences of macrophage apoptosis in atherosclerosis. J Lipid Res 2009;50 Suppl:S382–7.

KEY WORDS coronary artery disease, expansion index, intravascular ultrasound, lumen area, plaque area, vessel area

APPENDIX For an expanded Methods section and supplemental tables as well as supplemental videos and their legends, please see the online version of this article.